Electronic Supplementary Material (ESI) for Lab on a Chip.

Electronic Supplementary Materials for

Non-fouling polymer brush grafted fluorine-doped tin oxide enabled optical and chemical enhancement for sensitive label-free antibody microarrays

*Xiaoyi Li, Zhihao Feng, Changxiang Fang, Yunpeng Wei, Dandan Ji, and Weihua Hu**

Key Laboratory of Luminescence Analysis and Molecular Sensing (Southwest University), Ministry of Education; School of Materials and Energy, Southwest University, Chongqing 400715, P. R. China. Email: whhu@swu.edu.cn (W. Hu)

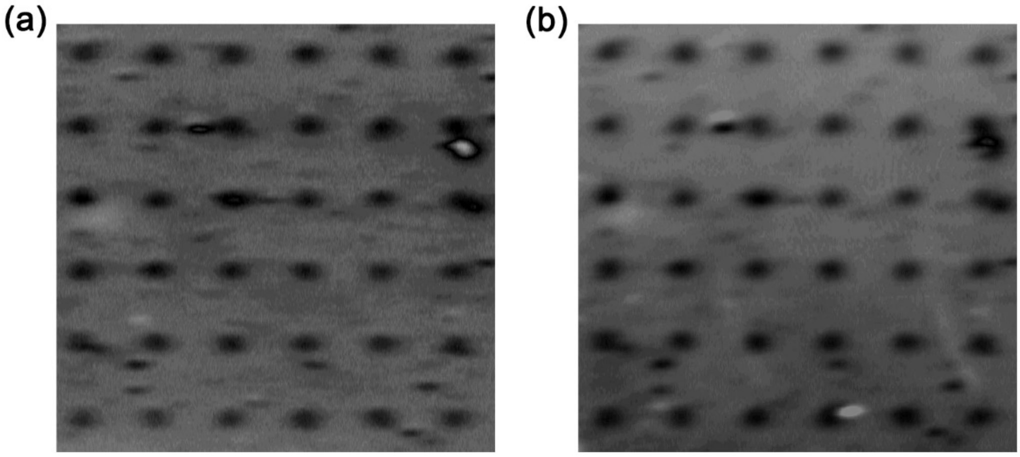

Fig. S1. OIRD images of microarray before (a) and after (b) reacting with 1 μg mL^{-1} CRP.

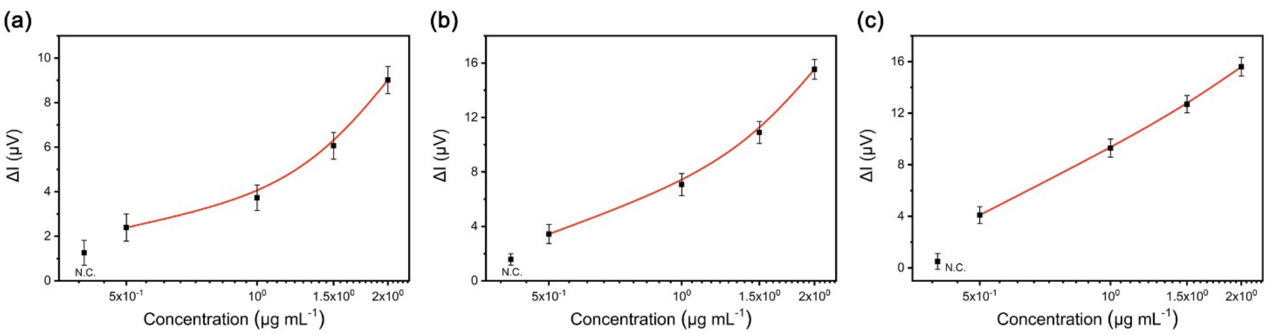

Fig. S2. Dose-response curve for detection of CRP on GPTES-glass (a), on GPTES-FTO (b) and on POEGMA-co-GMA-glass (c).

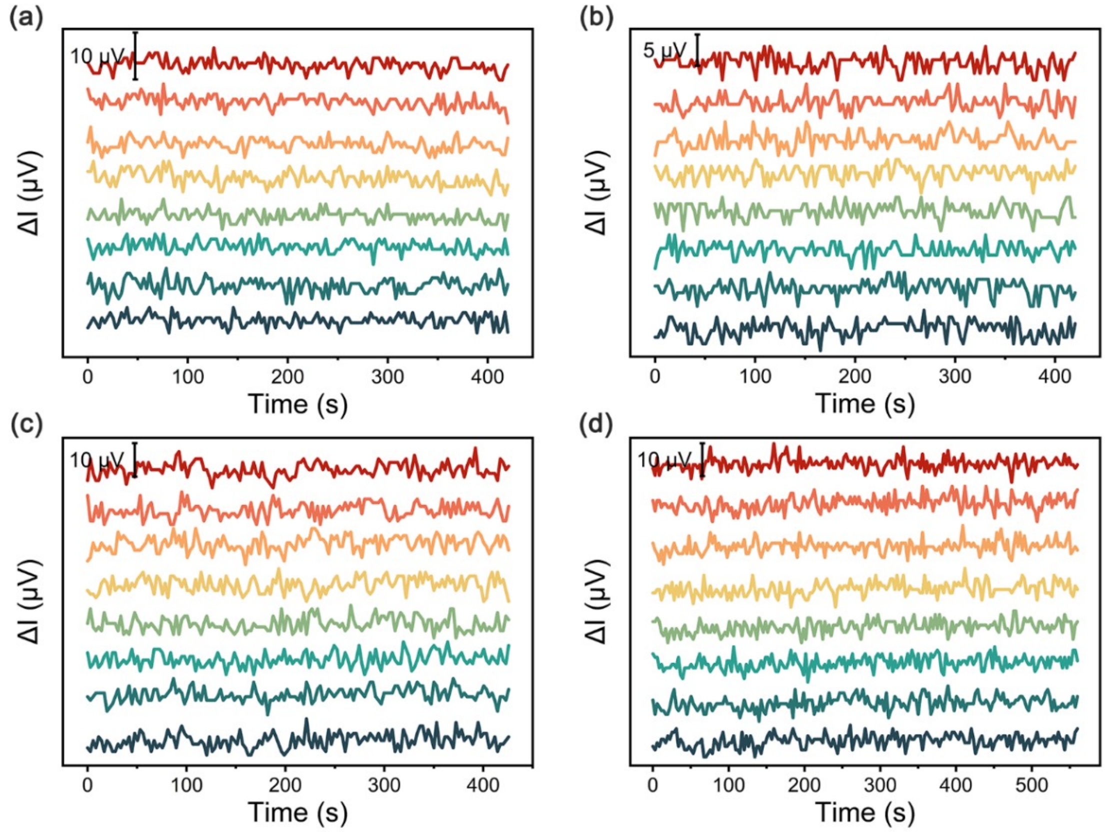

Fig. S3. *In situ* OIRD signals collected on POEGMA-co-GMA-FTO (a), POEGMA-co-GMA-glass (b), GPTES-FTO (c) and GPTES-glass (d) in 0.01 M PBS buffer. For each chip, the signals collected on 8 spots were shown.

Table S1. Thickness of POEGMA-co-GMA brush growth on FTO surface measured by ellipsometer.

Site	a	b	c	d	e
Thickness (nm)	58.11	58.56	57.96	59.11	58.31

Table S2. Performance of POEGMA-co-GMA brush based microarray for clinical samples.

Sample	Initial concentration (μg mL^{-1})[a]	Dilution multiples [b]	Measured concentration (μg mL^{-1}) [c]	Recovery (%) [d]
10E99	27	27	0.79	79.68
10E150	25.4	20	0.80	80.08

[a] the concentration determined by ELISA; [b] dilution multiple at which the sample was diluted before detecting with POEGMA-co-GMA-glass OIRD chip; [c] the concentration determined by POEGMA-co-GMA-glass OIRD chip; [d] Recovery = measured concentration × Dilution multiple / initial concentration × 100%.

Optical computation

OIRD achieves real time monitoring of surface/interface processes by measuring the time-lapsed difference between the relative changes in the reflectivity of p-polarized light and s-polarized light.

According to the OIRD principle, the OIRD signal of I(2Ω) from a certain interface is described by eqn (E1):

$$I(2\Omega) = I_0(|r_{p0}|^2\cos^2\alpha - |r_{s0}|^2\sin^2\alpha)J_2(A) \qquad \text{(E1)}$$

where Ω is the modulation frequency of the photoelastic modulator. I_0 is the initial light intensity of the laser. r_{p0} and r_{s0} are the p-polarized and s-polarized reflectivity of the surface, respectively. α is the angle between the optical axis of the polarization analyzer and the p-polarized light. $J_2(A)$ is the second kind Bessel function, where A is the amplitude of the modulation phase of the photoelastic modulator.

For microarray chips with functional layer, the reflective interface before detection can be described with a glass/functional layer/solution three-layer model (Figure 6a). The probe attached to the surface of the chip is treated as a part of the functional layer for simplification. ε_s, ε_p and ε_0 represent the dielectric constants of glass, functional layer and solution, respectively. φ_s, φ_p and φ_0 represent the angles of incidence in glass, functional layer and solution. h represents the thickness of functional layer.

The OIRD signal ($I_b(2\Omega)$) collected on the surface of the microarray chip before detection is described as:

$$I_b(2\Omega) = I_0(|r_{3p}|^2\cos^2\alpha - |r_{3s}|^2\sin^2\alpha)J_2(A) \qquad \text{(E2)}$$

Among them, r_{3p} and r_{3s} represent the reflectance of p-polarized light and s-polarized light at the functional layer/solution interface, respectively. $|r_{3p}|$ and $|r_{3s}|$ are the amplitudes of r_{3p} and r_{3s}.

After detection, the reflective interface can be described with a glass/functional layer/target/solution four-layer model (Figure 6a). The captured target biomolecules are scattered on the surface of the chip, which we have assumed to be a thin layer with an average thickness of d for analysis. ε_d and φ_d represent the dielectric constant and incident angle of the target protein, respectively.

Similarly, the OIRD signal ($I_a(2\Omega)$) collected on the surface of the microarray chip after detection can be described as:

$$I_a(2\Omega) = I_0(|r_{4p}|^2\cos^2\alpha - |r_{4s}|^2\sin^2\alpha)J_2(A) \qquad \text{(E3)}$$

Among them, r_{4p} and r_{4s} represent the reflectance of p-polarized light and s-polarized light at the target/solution interface, respectively. $|r_{4p}|$ and $|r_{4s}|$ are the amplitudes of r_{4p} and r_{4s}.

The ΔI(2Ω) signal originates from the glass/functional layer/solution three-layer to glass/functional layer /target/solution four-layer transformation. According to eqn (E1), the differential OIRD signal of ΔI(2Ω) could be calculated by subtracting the original $I_b(2\Omega)$ signal before detection from the final $I_a(2\Omega)$ signal after detection as follows:

$$\Delta I(2\Omega) = I_a(2\Omega) - I_b(2\Omega) = I_0[(|r_{4p}|^2 - |r_{3p}|^2)\cos^2\alpha - (|r_{4s}|^2 - |r_{3s}|^2)\sin^2\alpha]J_2(A) \quad \text{(E4)}$$

According to the Fresnel formula, the reflectivity of p-polarized light and s-polarized light in the glass/ functional layer /solution three-layer model respectively are:

$$r_{3p} = \frac{r_{sp}^{(p)} + r_{p0}^{(p)}e^{2i\psi_1}}{1 + r_{sp}^{(p)}r_{p0}^{(p)}e^{2i\psi_1}} \quad \text{(E5)}$$

$$r_{3s} = \frac{r_{sp}^{(s)} + r_{p0}^{(s)}e^{2i\psi_1}}{1 + r_{sp}^{(s)}r_{p0}^{(s)}e^{2i\psi_1}} \quad \text{(E6)}$$

Here,

$$\psi_1 = \frac{2\pi}{\lambda}h\sqrt{\varepsilon_p}\cos\varphi_p \quad \text{(E7)}$$

Among them, $r_{sp}^{(p)}$ and $r_{sp}^{(s)}$ represents the reflectance of p-polarized light and s-polarized light at the glass/functional layer interface, respectively. $r_{p0}^{(p)}$ and $r_{p0}^{(s)}$ represent the reflectance of p-polarized light and s-polarized light at the functional layer/solution interface, respectively.

According to the optical transmission matrix theory, the reflectivity of p-polarized light and s-polarized light in the glass/functional layer/target/solution four-layer model respectively are:

$$r_{4p} = \frac{r_{sp}^{(p)} + r_{pd}^{(p)}e^{2i\psi_1} + r_{d0}^{(p)}e^{2i(\psi_1+\psi_2)} + r_{sp}^{(p)}r_{pd}^{(p)}r_{d0}^{(p)}e^{2i\psi_2}}{1 + r_{sp}^{(p)}r_{pd}^{(p)}e^{2i\psi_1} + r_{sp}^{(p)}r_{d0}^{(p)}e^{2i(\psi_1+\psi_2)} + r_{pd}^{(p)}r_{d0}^{(p)}e^{2i\psi_2}} \quad \text{(E8)}$$

$$r_{4s} = \frac{r_{sp}^{(s)} + r_{pd}^{(s)}e^{2i\psi_1} + r_{d0}^{(s)}e^{2i(\psi_1+\psi_2)} + r_{sp}^{(s)}r_{pd}^{(s)}r_{d0}^{(s)}e^{2i\psi_2}}{1 + r_{sp}^{(s)}r_{pd}^{(s)}e^{2i\psi_1} + r_{sp}^{(s)}r_{d0}^{(s)}e^{2i(\psi_1+\psi_2)} + r_{pd}^{(s)}r_{d0}^{(s)}e^{2i\psi_2}} \quad \text{(E9)}$$

Here,

$$\psi_2 = \frac{2\pi}{\lambda}d\sqrt{\varepsilon_d}\cos\varphi_d \quad \text{(E10)}$$

Among them, $r_{pd}^{(p)}$ and $r_{pd}^{(s)}$ represents the reflectance of p-polarized light and s-polarized light at the functional layer/target interface, respectively. $r_{d0}^{(p)}$ and $r_{d0}^{(s)}$ represent the reflectance of p-polarized light and s-polarized light at the target/solution interface, respectively.

In general, the reflectivity of p-polarized light and s-polarized light at the a/b interface can be calculated by the following equation:

$$r_{ab}^{(p)} = \frac{\sqrt{\varepsilon_a}\cos\varphi_b - \sqrt{\varepsilon_b}\cos\varphi_a}{\sqrt{\varepsilon_a}\cos\varphi_b + \sqrt{\varepsilon_b}\cos\varphi_a} \qquad \text{(E11)}$$

$$r_{ab}^{(s)} = \frac{\sqrt{\varepsilon_a}\cos\varphi_a - \sqrt{\varepsilon_b}\cos\varphi_b}{\sqrt{\varepsilon_a}\cos\varphi_a + \sqrt{\varepsilon_b}\cos\varphi_b} \qquad \text{(E12)}$$

Among them, $r_{ab}^{(p)}$ and $r_{ab}^{(s)}$ represent the reflectance of p-polarized light and s-polarized light at the a/b interface of the substance. ε_a and ε_b represent the dielectric constants of substances a and b, respectively. φ_a and φ_b represent the angles of incidence in media a and b, respectively.

Substitute the equation E5-E12 into the equation E4, and ignore the initial light intensity I_0 and give the corresponding parameters, the variation law of the frequency-doubling signal intensity with the thickness of the functional layer can be calculated. Some parameters are assigned to facilitate the calculation: the wavelength of the incident laser λ=632.8 nm; the angle between the optical axis of the polarization analyzer and the p-polarized light α = π/2; the modulation frequency of the photoelastic modulator Ω=50 kHz; the amplitude of the modulation phase of the photoelastic modulator A=π; the refractive index of the glass slide $n_s = 1.50$; the refractive index of the solution $n_0 = 1.33$; the refractive index of FTO layer $n_p = 2.10$; the refractive index of the bound target protein $n = 1.5$.

The results shown in Fig. 7b are obtained by using different n_p and h for four chips. For GPTES-glass chip, use GPTES layer as the functional layer: $n_{p1} = 1.2$, $h_1 = 2\ nm$. For GPTES-FTO chip: $n_{p2} = 2.1$, $h_2 = 350\ nm$. For POEGMA-co-GMA-glass chip: $n_{p3} = 1.46$, $h_3 = 58\ nm$. For POEGMA-co-GMA-FTO chip: $n_{p4} = 1.976$, $h_4 = 58 + 350 = 408\ nm$.

We note that in this calculation, a single "functional layer" is used to model the FTO-brush layer for POEGMA-co-GMA-FTO chip to facilitate the four-layer model; a more accurate model should consider FTO and polymer brush as separated layers as their dielectric constants are different. Unfortunately the high-level five-layer calculation is complicated and we currently do not have the infrastructure and knowledge required for this simulation. Therefore, FTO-brush is treated as a single layer in POEGMA-co-GMA-FTO chip and its effective dielectric constant is calculated with the following formula:

$$\varepsilon_p = \frac{(h_a + h_b)\varepsilon_{pa} * \varepsilon_{pb}}{h_a * \varepsilon_{pb} + h_b * \varepsilon_{pa}} \qquad \text{(E13)}$$

Where, h_a and ε_{pa} are the thickness and dielectric constant of the first sensing layer, and h_b and ε_{pb} are the thickness and dielectric constant of the second sensing layer. For POEGMA-co-GMA-FTO based chip, the refractive index of POEGMA-co-GMA brush layer $n_{PEG} = 1.46$, and that of FTO layer $n_{FTO} = 2.10$. According to Formula E13, the refractive index of the sensing layer can be calculated as 1.976.

References including

(1) Li, X.; Fang, C.; Feng, Z.; Li, J.; Li, Y.; Hu, W. Label-free OIRD microarray chips with a nanostructured sensing interface: enhanced sensitivity and mechanism, *Lab Chip*, **2022**, 22 (20), 3910-3919

(2) Zhong, C.; Li, L.; Mei, Y.; Dai, J.; Hu, W.; Lu, Z.; Liu, Y.; Li, C. M.; Lu, H. B. Chip architecture-enabled sensitivity enhancement of oblique-incidence reflectivity difference for label-free protein microarray detection, *Sens. Actuators B Chem*., **2019**, 294, 216-223

(3) Dai, J. Label-free detection of biomolecular interactions by oblique incidence reflectivity difference method. PhD thesis, Institute of Physics, Chinese Academy of Sciences and The University of Chinese Academy of Sciences, **2014**

(4) Nagib, N. N.; Khodier, S. A. Applications of the Poincaré sphere in polarization metrology. *Opt. Laser. Technol.,* **2000,** *32* (5), 373-377

(5) Born, M.; Wolf, E. Principles of optics: electromagnetic theory of propagation, interference and diffraction of light, *Elsevier*, **2013**

(6) Zhu, X. D.; Fei, Y. Y.; Wang, X.; Lu, H. B.; Yang, G. Z. General theory of optical reflection from a thin film on a solid and its application to heteroepitaxy, *Phys. Rev. B*, **2007**, 75 (24).245434

(7) Liu, S.; Zhu, J. H.; He, L. P.; Dai, J.; Lu, H. B.; Wu, L.; Jin, K. J.; Yang, G. Z.; Zhu, H. Label-free, real-time detection of the dynamic processes of protein degradation using oblique-incidence reflectivity difference method, *Appl. Phys. Lett.*, **2014**, 104 (16).163701

(8) Zhu X D. Symmetry consideration in zero loop-area Sagnac interferometry at oblique incidence for detecting magneto-optic Kerr effects. *Rev. Sci. Instrum.,* **2017,** *88* (8).083112